High accuracy *ab initio* studies of Li_6^+, Li_6^-, and three isomers of Li_6

Berhane Temelso and C. David Sherrill[a)]
Center for Computational Molecular Science and Technology, School of Chemistry and Biochemistry, Georgia Institute of Technology, Atlanta, Georgia 30332-0400

(Received 17 August 2004; accepted 17 November 2004; published online 3 February 2005)

The structures and energetics of Li_6^+, Li_6^- and three isomers of Li_6 are investigated using the coupled-cluster singles, doubles and perturbative triples [CCSD(T)] method with valence and core-valence correlation consistent basis sets of double- to quadruple-ζ quality (cc-pVXZ and cc-pCVXZ, where X=D−Q). These results are compared with qualitatively different predictions by less reliable methods. Our results conclusively show that the D_{4h} isomer is the global minimum structure for Li_6. It is energetically favored over the C_{5v} and D_{3h} structures by about 5.1 and 7.1 kcal mol^{-1}, respectively, after the inclusion of the zero-point vibrational energy (ZPVE) correction. Our most accurate total atomization energies are 123.2, 117.6, and 115.7 kcal mol^{-1} for the D_{4h}, C_{5v}, and D_{3h} isomers, respectively. Comparison of experimental optical absorption spectra with our computed electronic spectra also indicate that the D_{4h} isomer is indeed the most stable structure. The cation, anion, and some higher spin states are investigated using the less expensive cc-pCVDZ basis set. Adiabatic ionization energies and electron affinities are reported and compared with experimental values. Predictions of molecular properties are found to be sensitive to the basis set used and to the treatment of electron correlation. © *2005 American Institute of Physics*. [DOI: 10.1063/1.1846671]

I. INTRODUCTION

There has been great interest in metal clusters over the past few decades due to the need to understand and explore the evolution of molecular properties with size.[1,2] Fascinating concepts like quantum confinement and surface effects in nanoclusters have captured the attention of scientists from all disciplines. Initially, the difficulties of producing clusters and characterizing them spectroscopically made computational and theoretical studies of these systems indispensable. Even as the experimental techniques have advanced, the role of computational studies in providing reliable geometries and energy levels for use in interpreting spectroscopic data has remained very significant.[1–6] Lithium clusters have been of special value in this endeavor due to their small number of electrons and the ease with which they can be studied using high-level computational methods.[7–12] The ultimate goal of these works is to understand the unique properties of these clusters as well as the evolution of their electronic structure as one starts with a single atom, builds clusters and nanoclusters, and finally reaches the bulk solid.[3,10]

Simple spherical shell models,[3,13] which assume that the valence electrons are independent and move in a spherically symmetric potential, have been very useful in gaining a qualitative understanding of the electronic structure of alkali metal clusters. The "jellium" model[2,14] improves upon this description by allowing the electrons to interact self-consistently within a local density approach. While this model has been applied successfully to sodium clusters,[2,15] it did not work as well for lithium clusters.[16,17] For example, the patterns in the sawtooth behavior of vertical ionization energies of lithium clusters with increasing size predicted by the jellium model diverged significantly from experiment,[16] and contrary to experimental results, the jellium model predicts lithium clusters to have more pronounced shell effects on dissociation energies than corresponding sodium clusters.[17] Some of the failures in the spherical jellium model have been attributed to the assumption of spherical electron density and subsequent theories including deviations from spherical symmetry have given more accurate predictions.[18,19] Also, these approaches do not treat core electrons explicitly and therefore may have difficulty when there is a small core-valence energy gap, as is the case with lithium. Additionally, deviations between density functional computations of bulk lithium using the local density approximation and experimental results for conductivity and Fermi surface-related properties[20,21] suggest that more sophisticated treatments of electron correlation may be important in describing lithium clusters reliably.

Lithium clusters of 2–40 atoms have been studied with density-functional theory (DFT) using both local density approximation (LDA) (Refs. 16 and 22) as well as nonlocal gradient-corrected functionals.[10,11,16,23] Koutecký *et al.* have used conventional *ab initio* electronic structure methods like Hartree–Fock (HF) and various types of configuration interaction (CI),[7–9,11,24] while others have used second-order Møller–Plesset perturbation theory (MP2),[11,25] coupled-cluster methods,[11,12] and complete active space self-consistent field theory (CASSCF).[11] McAdon and Goddard[26–28] used generalized valence bond (GVB) method to study metallic bonding in lithium clusters and proposed that valence electron density localizes in triangular sites for planar clusters and tetrahedral sites for three-dimensional species. *Ab initio* molecular dynamics,[29] *ab initio* path inte-

[a)]Electronic mail: sherrill@chemistry.gatech.edu

gral methods,[11,30,31] and variational quantum Monte Carlo[32] were among many other techniques[33,34] used to study these small clusters computationally.

The case of homonuclear metallic hexamers is a particularly rich and interesting one in that it is a transition point where planar and nonplanar isomers are competitive in energy. Clusters with less than 5–6 atoms generally prefer a planar conformation while those with six or more atoms take on three-dimensional structures.[4,6] This can be explained in terms of the minimization principle for the cluster surface area. While planar structures have less surface area for smaller clusters, a more compact 3D structure has less surface area for larger clusters. In the case of hexamers, the surface areas of the planar and 3D structures are competitive. The prominent structures for metal hexamers include a planar isomer with a triangular (D_{3h}) symmetry and two nonplanar isomers with pentagonal pyramidal (C_{5v}) and axially-compressed octahedral (D_{4h}) shapes. Looking at different metallic hexamers, the global minimum structure varies quite substantially. Additionally, different experimental and computational methods often indicate different structures. For example, geometric information on Au_6 derived from the vibrational autodetachment spectrum of Au_6^- initially suggested a ring structure of D_{6h} symmetry as a minimum[35] but it was later claimed that the C_{5v} isomer is the most stable structure.[36] More in-depth studies using theoretical methods like CASSCF, first- and second-order configuration interaction (FOCI and SOCI), and multireference diexcited configuration interaction (MRD-CI) concluded that the optimal structure of the gold hexamer is a capped pentagonal structure of C_{5v} symmetry.[37] Recent DFT studies have, however, predicted a planar triangular structure of D_{3h} symmetry.[38,39] Similar controversies have occured for Cu_6,[37,40,41] Ag_6,[37] and Na_6.[5,34,42]

For alkali-metal clusters, the presence of only an *s*-electron in the valence leads to two interesting phenomena. First, the bonding is not prone to directionality as is normally seen for clusters of atoms containing *p*- and *d*-electrons in their valence. Second, the potential energy surface becomes very flat and numerous shallow local minima appear. Both the absence of directional bonding as well as flat potential energy surfaces and shallow minima present challenges for experimentalists and theoreticians alike.[23] It thus comes as no surprise that there is a high level of ambiguity involving the optimal structure of Li_6.

For the case of Li_6, Hartree–Fock (HF) based *ab initio* molecular dynamics simulations showed that in three different 100 ps simulations, all three of the D_{4h}, C_{5v}, and D_{3h} isomers were sampled.[29] This is indicative of the flatness of the potential energy surface and the shallow nature of the minima. The D_{3h} isomer has received considerably more attention in earlier computational studies,[8,9,24] mainly because preceding works on the similar alkali metal cluster, Na_6, indicated that the D_{3h} structure was energetically favored over the other two isomers and because optical absorption spectroscopy on Na_6 gave results consistent with what would be expected from a D_{3h} cluster.[5] However, for Li_6, optical absorption spectra collected using depletion spectroscopy in the 400–700 nm range,[4,6] combined with minimal basis set

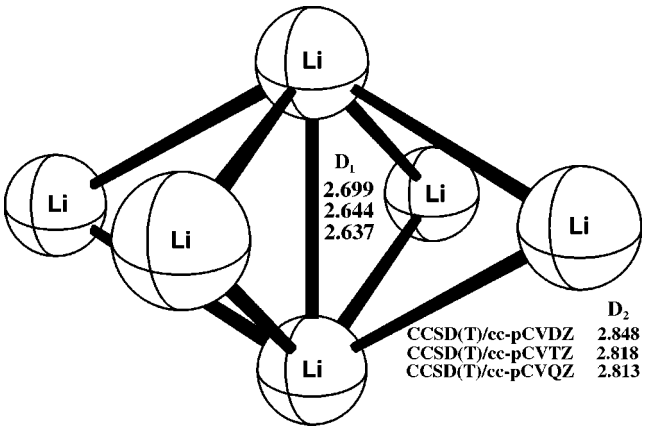

FIG. 1. D_{4h} isomer of Li_6.

MRD-CI (Ref. 9) computations, indicated a C_{2v} isomer. More recent theoretical studies using larger basis sets have found a more symmetric D_{4h} isomer but not the C_{2v} isomer.[10,11] The most reliable theoretical approach previously used to study Li_6 is quadratic configuration interaction with single and double excitations (QCISD), using a 6-311G* basis.[11]

There has been little experimental or theoretical work on the structures and properties of anionic and cationic lithium hexamers. Li_6^+ has been observed after lithium vapor aggregates into clusters and the product is ionized by a powerful laser.[4,6] Some theoretical work on the cationic and anionic lithium hexamer has been performed by using the SCF and MRD-CI methods,[24] but only a minimal basis set was used.

In this work, we present highly accurate geometries, zero-point vibrational energies (ZPVE's), and binding energies in order to resolve the uncertainty concerning the relative stability and energetics of the three isomers of Li_6 (D_{4h}, C_{5v}, and D_{3h}), shown in Fig. 1–3. Our best estimates of the binding energies use the very reliable coupled-cluster method with single, double, and perturbative triple substitutions [CCSD(T)] (Ref. 43) in conjunction with a very large basis set, the quadruple-ζ polarized core-valence basis set cc-pCVQZ. These results should closely approach the *ab initio* limit for these isomers. We also report the first high-level theoretical results for the lowest $^3B_1$ state of Li_6 (Fig. 4) and the ground states of Li_6^+ (Fig. 5) and Li_6^- (Fig. 6). Due to the

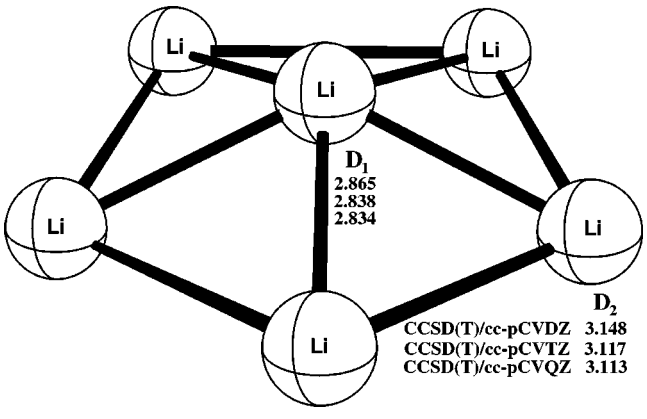

FIG. 2. C_{5v} isomer of Li_6.

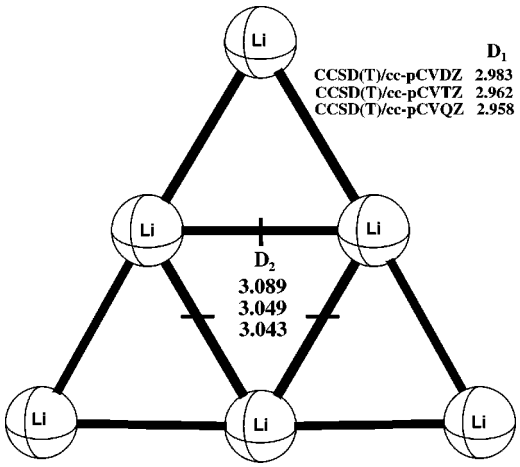

FIG. 3. D_{3h} isomer of Li_6.

open-shell nature of these species, computations are more difficult, and so we use the more modest cc-pCVDZ basis. The effects of basis sets and electron correlation are also carefully investigated for these clusters.

II. COMPUTATIONAL APPROACH

All computations were carried out using the ACES II (Ref. 44) and MOLPRO (Ref. 45) program packages running on a 72-processor IBM SP and a 48-processor IBM Pentium 4 Linux cluster. Geometry optimizations were done using analytic gradient methods employing the rational-function approximation (RFA) technique in ACES II. For geometric optimizations of the singlet state at the CCSD(T)/cc-pCVQZ level, numerical gradients with the RFA method were used, as implemented in MOLPRO. All frequencies and ZPVE's have been computed using ACES II at the CCSD(T)/cc-pCVDZ level of theory. Plots of Hartree–Fock valence orbitals were generated using the cc-pCVDZ basis with MOLDEN's (Ref. 46) interface to MOLPRO. Vertical excitation spectra for the singlet states are computed using equation-of-motion (EOM) CCSD.[47]

The unusual bonding in these clusters raises the question of whether single-reference methods, based upon the assumption of a single dominant electron configuration, are appropriate. Previous investigation[11] of the CASSCF one-particle density matrix indicated that single-reference approaches suffice for these clusters. It was found that the

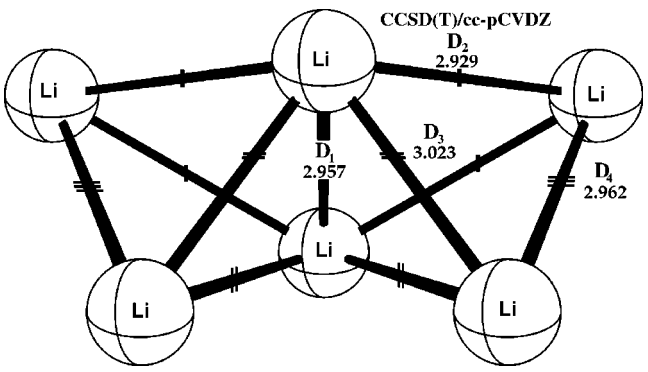

FIG. 4. The structure of the $^3B_1$ state of Li_6 (C_{2v} symmetry).

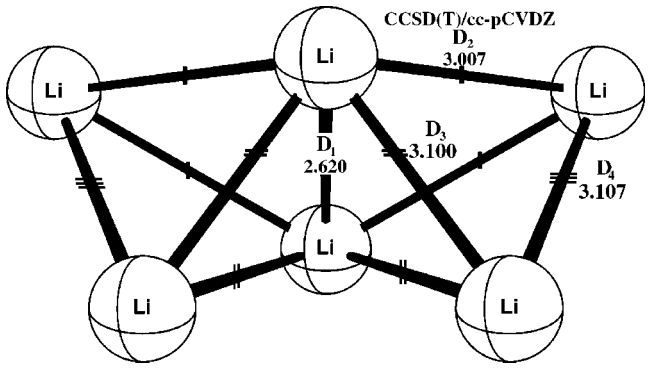

FIG. 5. The structure of Li_6^+ (C_{2v} symmetry).

CASSCF wave function is built mostly (92% for Li_2 and 93% for Li_3^+) from the reference Hartree–Fock determinant. We computed the T_1 diagnostic (Refs. 48 and 49) at the CCSD(T)/cc-pCVQZ level and obtained 0.013, 0.012, and 0.011 for the D_{4h}, C_{5v}, and D_{3h} structures, respectively. These values are all below the recommended 0.020 threshold above which multireference character and nondynamical correlation often become significant. Additionally, the magnitudes of the largest T_2 amplitudes for these isomers (0.065, 0.074, and 0.062 for D_{4h}, C_{5v}, and D_{3h}) compare favorably with the largest T_2 amplitudes for systems like H_2O and BH which contain very little multireference character (e.g., the largest T_2 for CCSD/6-31G* H_2O is 0.052). For Li_6^+ and Li_6^-, the largest T_2 amplitudes at the CCSD(T)/cc-pCVDZ level of theory had magnitudes of 0.072 and 0.077, respectively. We therefore expect the CCSD(T) method to yield accurate results for these systems.

We use the correlation consistent basis sets of Dunning and co-workers[50–54] because they yield energies and properties that converge systematically towards the complete basis set (CBS) limit. These basis sets include polarization functions which can be critical in describing systems with significantly delocalized electron densities.[24] Because the 1*s* and 2*s* electrons in lithium atom are similar in energy, core correlation can be important also, and thus all electrons need to be correlated. However, standard split-valence basis sets lack

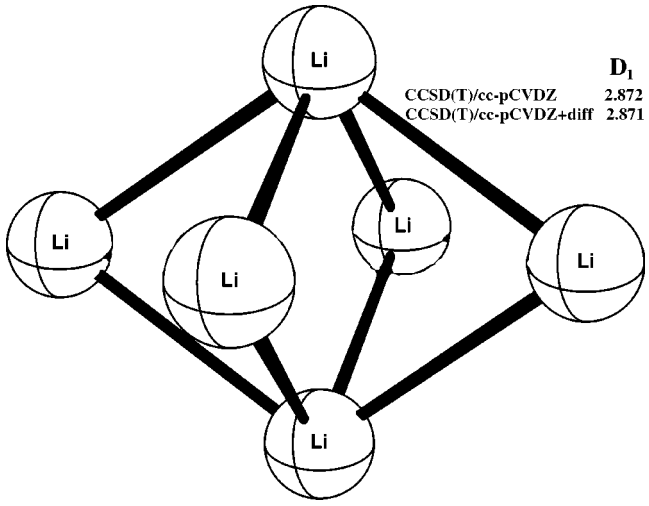

FIG. 6. The structure of Li_6^- (D_{4h} symmetry).

tight core functions appropriate to describe core correlation, and this can be particularly problematic for alkali earth metals such as lithium.[55] Indeed, for the standard cc-pV*X*Z basis sets, we observed significant jumps in predicted geometries and energies as progressively larger basis sets were used. For this reason, we have also employed the core-valence correlation consistent basis sets (cc-pCV*X*Z) of Dunning and co-workers,[51] as well as the related "core-valence weighted" (cc-pwCV*X*Z) (Refs. 12 and 56) basis sets. These basis sets are compared in Sec. III A. For the anionic lithium hexamer, Li_6^-, diffuse functions may also be important. However, there are no correlation consistent basis sets with diffuse functions for alkali and alkaline metals. To circumvent that problem, we added the diffuse *s* and *p* functions from the 6-311++G** basis set[57] to the standard core-valence correlations consistent basis sets (cc-pCV*X*Z).

The *ab initio* atomization energy or binding energy per atom is indicative of the "static stability" of the clusters, while the "dynamic stability," which is not computed here, corresponds to the relative stability of clusters of different sizes and is thus useful in determining fragmentation and dissociation pathways, cascading to an ultra-stable cluster with a "magic number" of atoms.[4,58] The binding energies per atom (E_b^6, E_b^{6+}, and E_b^{6-}) can be computed from the energy of the hexamer (E_6, E_6^+, and E_6^-) and the energies for the neutral (E_1), cationic (E_1^+) and anionic (E_1^-) lithium atom as follows:

$$E_b^6 = (6E_1 - E_6)/6, \tag{1}$$

$$E_b^{6+} = (5E_1 + E_1^+ - E_6^+)/6, \tag{2}$$

$$E_b^{6-} = (5E_1 + E_1^- - E_6^-)/6. \tag{3}$$

Due to the closeness in energy between the three isomers in this study, it is essential to include a zero-point vibrational energy (ZPVE) correction to the Born–Oppenheimer energies. We have computed ZVPE's at the CCSD(T)/cc-pCVDZ level of theory. Using larger basis sets for ZPVE's becomes very difficult because of the large computational expense involved in obtaining second derivatives. Second derivatives were also used to perform vibrational frequency analysis to verify the character of optimized geometries as minima or saddle points. Adiabatic ionization energies have been calculated for the neutral clusters at the CCSD(T)/cc-pCVDZ level. The equation-of-motion CCSD (EOM-CCSD) (Ref. 47) method, as implemented in ACES II,[44] is currently the state-of-the-art technique for predicting electronic excited state properties and it is used here to determine vertical excitation energies and oscillator strengths. The theoretical spectra predicted by EOM-CCSD are compared with experimental spectra[4,6] to determine which isomer is observed experimentally at low temperatures.

III. RESULTS AND DISCUSSION

A. Basis set effects

As discussed previously, finding a good correlation consistent basis set for lithium is critical for predicting properties reliably. The conventional valence-only correlation consistent basis sets (cc-pV*X*Z), which are designed for frozen-core calculations, are not convenient for systems containing atoms with a small core-valence energy separation. Instead, it is important to use basis sets including core correlating functions, such as the correlation consistent core-valence (cc-pCV*X*Z) sets. In order to check the reliability of the different correlation consistent basis sets, we performed tests to see which basis sets yield a monotonic and smooth convergence for different properties, particularly geometries and binding energies. Table I and Fig. 7 compare the change in predicted geometries and energies for the D_{4h} isomer as we use the cc-pV*X*Z, cc-pCV*X*Z, and cc-pwCV*X*Z basis sets of increasing cardinal numbers *X*. The bond lengths, D_1 and D_2, are defined in Figs. 1–3. For the case of the valence-only (cc-pV*X*Z) basis sets, there is a large change in predicted geometry (−0.131 Å for D_1 and −0.080 Å for D_2) and binding energy per atom (1.96 kcal mol^{-1}) upon going from cc-pVDZ to cc-pVTZ. The change for cc-pVTZ to cc-pVQZ is still large but a little less pronounced both in terms of geometries and binding energies. In contrast, the core-valence basis sets (cc-pCV*X*Z) show a much smaller jump in geometries (−0.055 Å for D_1 and −0.029 Å for D_2) and binding energies (0.77 kcal mol^{-1}) for a change from cc-pCVDZ to cc-pCVTZ. The difference is even smaller, as it should be, for a change from cc-pCVTZ to cc-pCVQZ: −0.007 Å for D_1, −0.006 Å for D_2, and 0.19 kcal mol^{-1} for the binding energy. The significant change in the geometry and binding energies computed using the cc-pV*X*Z basis sets demonstrates that the one-particle space it represents is converging slowly while the much smaller change for the cc-pCV*X*Z basis sets is indicative of a representation that is approaching completeness at a faster rate. We performed a similar analysis of the core-valence weighted correlation consistent basis sets (cc-pwCV*X*Z), which are designed to more rapidly converge the core-valence correlation energy at the expense of the core-core correlation energy.[56] For Li_6, we found very

TABLE I. Changes to energies and bond lengths with respect to changes in basis set for the D_{4h} isomer.

Level of theory	Bond length (Å) D_1	Bond length (Å) D_2	Binding energy[a] per atom
Basis set effects			
cc-pV*XZ*			
VTZ-VDZ	−0.131	−0.080	1.96
VQZ-VTZ	−0.033	−0.066	1.72
cc-pCV*XZ*			
CVTZ-CVDZ	−0.055	−0.029	0.77
CVQZ-CVTZ	−0.007	−0.006	0.19
cc-pwCV*XZ*			
wCVTZ-wCVDZ	−0.053	−0.029	−0.75
Correlation effects			
[*CCSD(T)-CCSD*]/VDZ	0.053	−0.002	0.95
[*CCSD(T)-CCSD*]/VTZ	0.039	−0.007	1.14
[*CCSD(T)-CCSD*]/CVDZ	0.046	−0.004	1.02

[a]In kcal mol^{-1}.

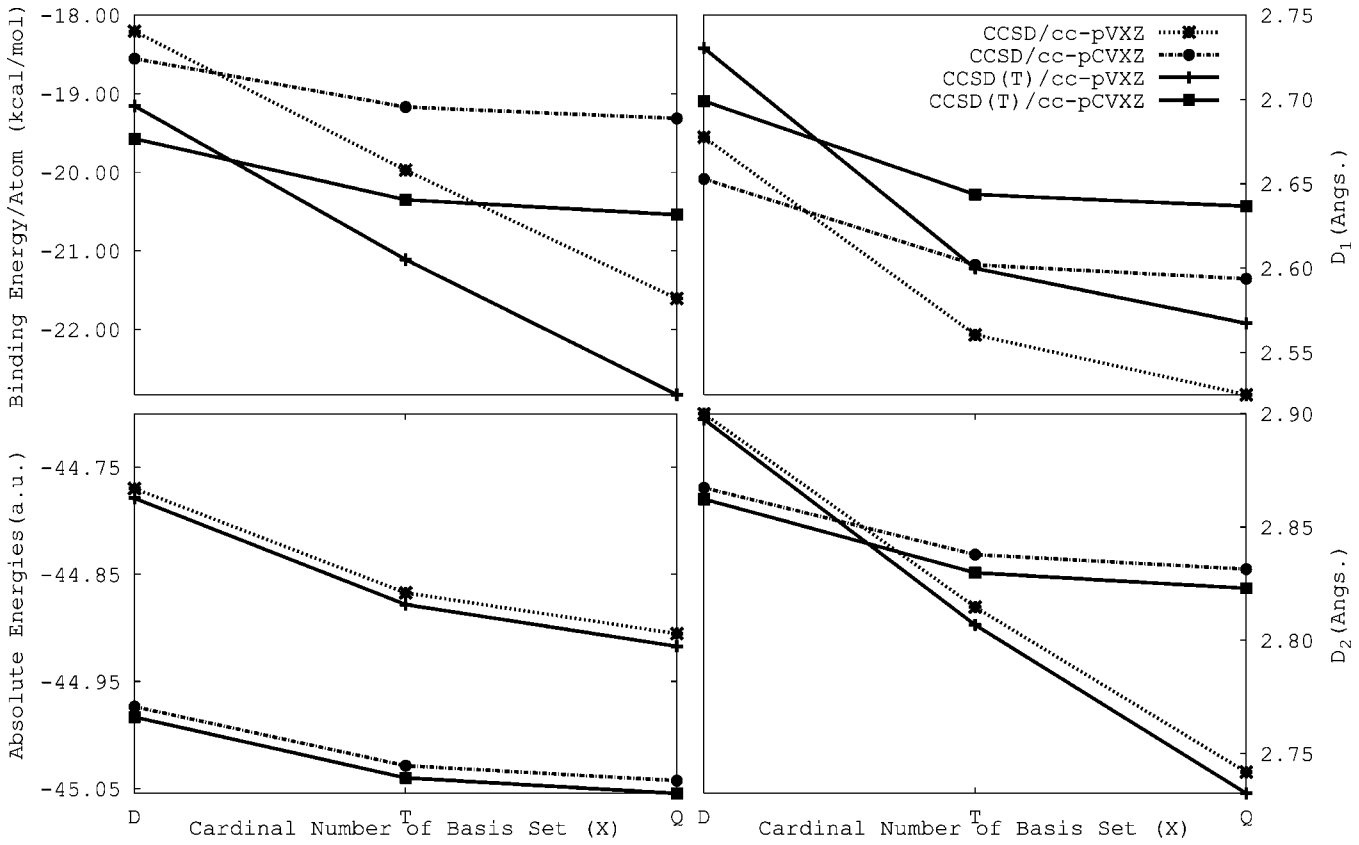

FIG. 7. Comparison of correlation and basis set effects for the D_{4h} isomer of Li_6.

little difference between the cc-pCV*X*Z and cc-pwCV*X*Z basis sets, and thus we used the former in the remainder of the study.

B. Electron correlation effects

One of the challenges of *ab initio* electronic structure theory is to find a highly accurate yet computationally feasible compromise between the level of electron correlation (*n*-particle space, where *n* is the number of electrons) and the size of the basis set (one-particle space).[59] Table I compares the effect of changing the correlation treatment from CCSD to CCSD(T) with that of increasing the size of basis set for the D_{4h} isomer. This information is also displayed in Fig. 7, which demonstrates that basis set incompleteness, core correlation, and triple excitations can *all* be important in obtaining accurate results. Therefore, we employ CCSD(T), core electrons being correlated, with the largest basis set feasible at each stage of our predictions. Our best energies for Li_6 are computed with the large cc-pCVQZ basis. More expensive computations of frequencies and of open-shell Li_6^+ and Li_6^- employ the cc-pCVDZ basis.

C. Singlet state of Li_6

As noted previously, the singlet state of Li_6 has three energetically close isomers: D_{4h}, C_{5v}, and D_{3h}.[29] Each one of these isomers corresponds to a local minimum on the potential energy hypersurface, as verified here by normal mode analysis. To check for the existence of other local minima, we performed calculations using a much lower spatial symmetry (C_s), but all those attempts led back to a structure matching one of the three isomers discussed here. It has been suggested that D_{5h} and C_{2v} isomers exist; however, optimizations starting from a D_{5h} configuration lead back to the quasiplanar C_{5v} isomer, and the C_{2v} structure changes to a more symmetric D_{4h} isomer upon using a larger basis set and a more complete correlation method.

A brief synopsis of relative energies predicted in previous literature for the three isomers is given in Table II. One of the first treatments is a minimal basis HF computation which predicts a D_{3h} global minimum. Multireference diexcited configuration interaction, with and without Davidson correction (MRD-CI-Dav and MRD-CI, respectively), suggest a C_{5v} isomer as the most stable species.[24] These discrepancies are indicative of the sensitivity of Li_6 geometries and energies to the basis set and correlation method used. Other computations by Rousseau *et al.*[11] using a triple-ζ basis set and a variety of correlated methods predict a D_{4h} global minimum even though the relative energies vary quite significantly and the ordering of the other two isomers differs depending on the methods used. For example, while the QCISD method suggests a more stable D_{3h} structure than a C_{5v} one, MP2 and B3LYP predict otherwise. It is also worth noting that the HF method using minimal basis gives completely different results from HF/6-311G*, once again showing the importance of basis set effects in these systems.

1. D_{4h} isomer

Early works in the literature[7–9,24] have claimed that a minimum of C_{2v} symmetry exists, while more advanced

TABLE II. Comparison of different methods from previous literature.

Method	Relative energy (kcal mol^{-1})		
	D_{4h}/C_{2v}	C_{5v}	D_{3h}
HF/MB[a,b]	5.40	4.32	0.00
HF/6-311G[d]	0.00	2.62	1.31
MRD-CI/MB[a,b]	1.74	0.00	0.30
MRD-CI-Dav/MB[a–c]	2.10	0.00	0.24
QCISD/6-311G[d]	0.00	3.82	2.81
B3LYP/6-311G[d]	0.00	3.72	5.32
MP2/6-311G[d]	0.00	5.03	7.66

[a]Minimal basis, see Ref. 24 for details.
[b]Calculated from binding energies provided in Ref. 24.
[c]MRD-CI with Davidson correction, see Ref. 24 for details.
[d]See Ref. 11.

methods have later shown that the C_{2v} isomer in fact is an axially-compressed octahedral structure of D_{4h} symmetry.[10,11] It has two types of bonds, namely a shortened axial bond, designated as D_1 in Fig. 1, and another slightly longer bond, labeled as D_2. As shown in Table III, the most accurate bond lengths for D_1 and D_2 are 2.637 Å and 2.813 Å at the CCSD(T)/cc-pCVQZ level. These values are well-converged, as can be seen by the small changes (−0.007 Å and −0.006 Å in D_1 and D_2, respectively), upon going from the cc-pCVTZ to the cc-pCVQZ basis. Binding energies also appear well-converged at the CCSD(T)/cc-pCVQZ level, which predicts 123.24 kcal mol^{-1} (total) and 20.54 kcal mol^{-1} (per atom). (Table III also includes total energies for easier reproducibility of our theoretical results.)

We can guage the level of oblateness in the D_{4h} isomer by taking the ratio of its rotational constant with respect to the compressed axis (0.097 cm^{-1}) with that along the uncompressed axes (0.152 cm^{-1}). While this ratio should be 1.00 for an octahedron, the value for our D_{4h} isomer at the CCSD(T)/cc-pCVQZ level is 1.567. The energetic advantage of this distortion away from O_h symmetry is assessed by comparing the energy of a cluster constrained to be perfectly octahedral with that allowed to relax into a D_{4h} minimum. Accordingly, at the CCSD(T)/cc-pCVDZ level of theory, we find that a cluster constrained to an O_h symmetry is 12.4 kcal mol^{-1} higher in energy than that allowed to distort to D_{4h} symmetry.

TABLE III. Singlet state isomers of Li_6.

Level of theory	Energy (a.u.)	Bond length (Å)		ZPVE[a]	Binding energy[a]		Relative energy[a,b]
		D_1	D_2		Total	per atom	
D_{4h}							
CCSD(T)/cc-pVDZ	−44.778 989	2.730	2.879	3.60	114.94	19.16	0.00(0.00)
CCSD(T)/cc-pVTZ	−44.878 263	2.600	2.798	3.85	126.67	21.11	0.00(0.00)
CCSD(T)/cc-pVQZ	−44.917 279	2.567	2.732		137.00	22.83	0.00(0.00)
CCSD(T)/cc-pCVDZ	−44.983 317	2.699	2.848	3.71	117.45	19.58	0.00(0.00)
CCSD(T)/cc-pCVTZ	−45.040 081	2.644	2.819		122.11	20.35	0.00(0.00)
CCSD(T)/cc-pCVQZ	−45.054 531	2.637	2.813		123.24	20.54	0.00(0.00)
C_{5v}							
CCSD(T)/cc-pVDZ	−44.772 879	2.898	3.169	3.18	111.10	18.52	3.83(3.42)
CCSD(T)/cc-pVTZ	−44.867 203	2.819	3.095	3.19	119.73	19.96	6.94(6.27)
CCSD(T)/cc-pCVDZ	−44.976 566	2.865	3.148	3.23	113.21	18.87	4.24(3.75)
CCSD(T)/cc-pCVTZ	−45.031 248	2.838	3.117		116.57	19.43	5.54(5.06)
CCSD(T)/cc-pCVQZ	−45.045 571	2.834	3.113		117.62	19.60	5.62(5.14)
D_{3h}							
CCSD(T)/cc-pVDZ	−44.770 865	3.016	3.130	3.16	109.84	18.31	5.10(4.66)
CCSD(T)/cc-pVTZ	−44.863 290	2.950	3.029	3.20	117.28	19.55	9.40(8.75)
CCSD(T)/cc-pCVDZ	−44.974 510	2.983	3.089	3.21	111.92	18.65	5.53(5.03)
CCSD(T)/cc-pCVTZ	−45.028 196	2.962	3.049		114.65	19.11	7.46(6.96)
CCSD(T)/cc-pCVQZ	−45.042 434	2.958	3.043		115.65	19.28	7.59(7.09)

[a]In kcal mol^{-1}.
[b]ZPVE corrected results given in parentheses.

2. C_{5v} isomer

The C_{5v} structure has a pentagonal pyramidal shape with a short C_5 axis. The distance between the base of the pentagon and the out-of-plane lithium atom is small ($\sim$1.0 Å), indicating the quasiplanar nature of this isomer. There is a very small energy separation [1.95 kcal mol^{-1} at the CCSD(T)/cc-pCVQZ level with CCSD(T)/cc-pCVDZ ZPVE correction] between the quasiplanar C_{5v} isomer and the planar D_{3h} structure, the C_{5v} isomer being more stable.

The geometric parameters reported for this isomer are the distance between any atom in the pentagonal base and the out-of-plane lithium atom, designated as D_1, and the other bond between any two adjacent lithium atoms on the pentagonal base, designated as D_2. Our most accurate predictions at the CCSD(T)/cc-pCVQZ level of theory are D_1 = 2.834 Å and D_2 = 3.113 Å. The total and per-atom binding energies at this level are 117.62 kcal mol^{-1} and 19.60 kcal mol^{-1}, respectively, and this isomer lies 5.14 kcal mol^{-1} above the D_{4h} isomer after ZPVE correction. The rotational constant with respect to the two equivalent axes on the pentagonal base are 0.131 cm^{-1}, in contrast to 0.069 cm^{-1} along the short C_5 axis.

3. D_{3h} isomer

Hexamers composed of larger atoms, notably Na_6,[5,7,42,60] Cu_6,[37,40,41] Ag_6,[37] and Au_6,[38] have been found to have planar D_{3h}-type structures as their most stable form, and the case of the lithium hexamer is considered peculiar for that reason. The main reason why the D_{3h} isomer is energetically favorable in hexamers of larger atoms as opposed to the case of lithium hexamers is under investigation.

The D_{3h} isomer is not perfectly triangular as the inner triangular structure exhibits a slightly different three-center bonding than do the outer bonds. As a result, the outer bonds, designated as D_1, are slightly smaller than the inner three-center bonds labeled as D_2. Similar geometries have been predicted in previous studies of this isomer.[6,11] Our CCSD(T)/cc-pCVQZ computations give 2.958 Å and 3.043 Å for D_1 and D_2, respectively. The total and per-atom binding energies at this level are 115.65 and 19.28 kcal mol^{-1}, respectively. The corresponding rotational constants are 0.109 cm^{-1} with respect to the two equivalent axes in the plane of the molecule and 0.054 cm^{-1} with respect to the C_3 axis perpendicular to the plane of the molecule.

4. Comparison and analysis

As noted earlier, the presence of only one valence *s* electron in alkali metal atoms gives birth to nondirectional bonding in clusters. A more in-depth study of bonding in lithium clusters has been performed by Rousseau and co-workers,[10,11] who used density-functional theory (DFT) and electron localization functions (ELF). It was found that electrons in lithium clusters localize in interstitial regions, leading to multicenter bonding. For smaller clusters, this multicenter bonding leads to "bond alternation" in the range of 2.45–3.15 Å. The bond alternation occurs between a "short" two-center two-electron (2*c*-2*e*) type, characteristic of Li_2, the "long" three-center two-electron (3*c*-2*e*) bond prototypical of triangular Li_3^+ and other multicenter *n*-electron bonds. The "short" bond has a length that ranges from 2.45 Å to 2.85 Å while the "long" three/four-center type of bond has a length of 2.85–3.15 Å.[10,11] As shown in Table III, the D_{4h} isomer exhibits a short axial bond (2.637 Å) and long axial-to-equatorial bonds (2.813 Å) at the most complete level of theory. The C_{5v} structure exhibits long bonds (3.113 Å) between adjacent atoms in the pentagonal base and intermediate bond lengths (2.834 Å) between the cap and the pentagonal base. The D_{3h} structure exhibits only the three-center two-electron bonding with Li–Li bond lengths of 2.958–3.043 Å.

The stability of the clusters can be studied by examining the binding energies (atomization energies) as well as the relative energies of the different isomers with respect to the most energetically favorable isomer, D_{4h}. As shown in Table III, the binding energy per atom at the CCSD(T)/cc-pCVQZ level is 20.54 kcal mol^{-1} (0.89 eV), 19.60 kcal mol^{-1} (0.85 eV), and 19.28 kcal mol^{-1} (0.84 eV) for the D_{4h}, C_{5v}, and D_{3h} isomers, respectively. Relative to the D_{4h} isomer, the C_{5v} and D_{3h} isomers lie 5.14 kcal mol^{-1} and 7.09 kcal mol^{-1} higher in energy, respectively, after ZPVE correction. This level of theory should be sufficient to predict these energies very accurately. Based on the observed convergence of results and the typical reliability of the methods employed, we expect errors within ±0.5 kcal mol^{-1} for relative energies and ±0.1 eV for binding energies. Thus we expect that the present results are sufficiently accurate to definitively determine the energetic ordering of the three isomers. However, it is also interesting to compare our predictions to the available experimental data. Bréchignac *et al.*[17] have combined their experimental ionization potential of Li_6 [IP(Li_6)] and Li [IP(Li)],[61] with the binding energy of Li_6^+ [$E_b(Li_n^+)$], determined using unimolecular dissociation of ionized clusters to give an experimental atomization energy of 0.88 eV per atom for Li_6:

$$E_b(\mathrm{Li}_6) = E_b(\mathrm{Li}_6^+) + \mathrm{IP}(\mathrm{Li}_6) - \mathrm{IP}(\mathrm{Li}). \quad (4)$$

The binding energy of 0.89 eV per atom we predicted for the D_{4h} isomer agrees with the experimental value best, but given our estimated error bars of about ±0.1 eV and those entailed in the indirect determination of the experimental atomization energy, the comparison is inconclusive.

Rousseau[10] has suggested that the D_{4h} isomer is more stable because the axial lithium atoms contain two orthogonal *p* orbitals which can produce π-type interactions. Looking at the plots of the valence orbitals for these isomers in Figs. 8–10 elucidates some of the predicted structural features. As shown in Fig. 8, the HOMO-2 orbital for the D_{4h} isomer has most of its electron density along the compressed axis and the HOMO-1 and HOMO orbitals effectively contribute to give the compressed bond a conventional "triple bond" character. Equally insightful are the valence orbital plots for the other two isomers, where we see the localization of most of the valence electron density over the interstitial regions. The similarity in the electron density of the D_{3h} and C_{5v} isomers can explain previous studies[4] which suggested that while there is a small energy barrier separating the non-

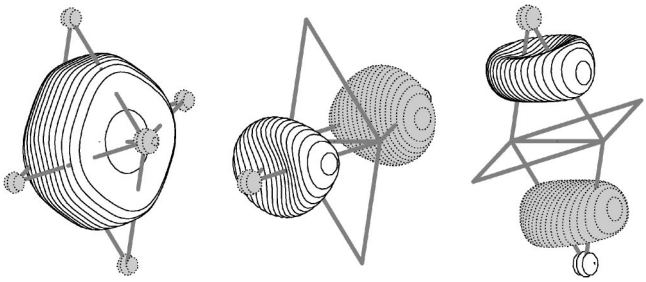

FIG. 8. HOMO-2, HOMO-1, and HOMO for the D_{4h} isomer of Li_6.

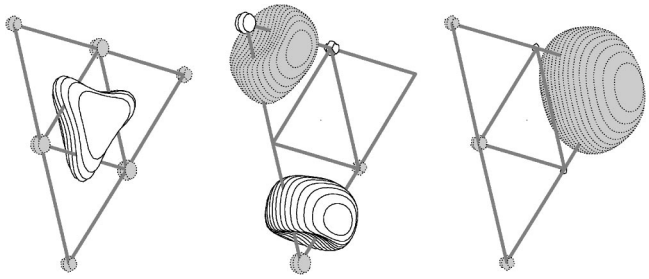

FIG. 10. HOMO-2, HOMO-1, and HOMO for the D_{3h} isomer of Li_6.

planar D_{4h} isomer from the D_{3h} isomer, the quasiplanar C_{5v} converts to the D_{3h} structure without a barrier by displacing its out-of-plane atom into the pentagonal base. The energy difference between the D_{3h} and C_{5v} isomers is only 1.95 kcal mol^{-1}.

While there are no direct experimental determinations of geometrical parameters like bond lengths and angles for comparison with our theoretical values, optical absorption spectra[4,6] combined with *ab initio* vertical excitation spectra can yield qualitative understanding of the structure of these clusters. Depletion spectroscopy in the range of 400–700 nm has been used to produce the spectrum given in Fig. 11. It is dominated by two features, namely a small peak at 1.8 eV and a more intense peak at 2.5 eV. The clusters produced in these experiments undergo cooling coexpansions in vacuum with 1–5 bars of argon gas, achieving low internal vibrational tempeatures: 70 K for Li_2, 25 K for Li_3, and much lower temperatures for larger clusters with significantly more degrees of freedom.[4,6] Previous investigations[30,31] on structural changes of lithium clusters due to quantum and thermal fluctuations have concluded that while such fluctuations do lead to the disappearance of bond alternation, they do not lead to isomerization reactions at these temperatures. Therefore, qualitative comparisions between the above-mentioned optical absorption spectra and calculated vertical excitation spectra from static *ab initio* techniques are justified.

To investigate which isomer gives an electronic spectrum containing similar features, we calculated vertical electronic excitation energies and oscillator strengths for each isomer at the EOM-CCSD/cc-pCVDZ level of theory. The results are displayed in Fig. 12, in which the lines have been broadened artificially using Lorentzian functions centered about intense peaks to simulate a real spectrum and simplify the comparison with the experimental spectrum (no actual computations of linewidths were performed). The figures indicate that, within the errors of the EOM-CCSD (typically ±0.3 eV for excitation energies), the features in the spectrum of the D_{4h} isomer match the experimental spectra best. The pronounced peaks in the D_{4h} spectrum appear at 1.7 and 2.6 eV, compared to 1.8 and 2.5 eV in the experimental spectrum. In contrast, the C_{5v} spectrum has only one sharp peak at 2.2 eV, while the D_{3h} isomer has two small peaks at 1.7 and 2.8 eV and a pronounced one at 2.2 eV. Thus the experimental spectrum appears to match best the computed spectrum of the D_{4h} isomer, consistent with our very accurate results for the energetics which demonstrate that this isomer is the most stable and should be the most heavily populated at the low temperatures of the experiment.[6] However, we can not rule out the possibility that other isomers contributed to the observed optical absorption spectrum. We note that previous computations of the absorption spectrum using the MR-CISD method provided similar results,[4,6] although those computations yielded additional peaks which have very small oscillator strengths according to our computations.

If we compare the previous, lower-level theoretical results in Table II to our present high-level results, we see that all of the minimal basis set results, even those with extensive electron correlation, predict the wrong energetic ordering of the isomers. As for the 6-311G* predictions of Rousseau and Marx,[11] Hartree–Fock and QCISD give the wrong energetic ordering, while B3LYP and MP2 give the correct energetic ordering of the isomers. The MP2/6-311G* relative energies are quite close (within 0.7 kcal mol^{-1}) to the best present coupled-cluster results. Given the significant correlation and

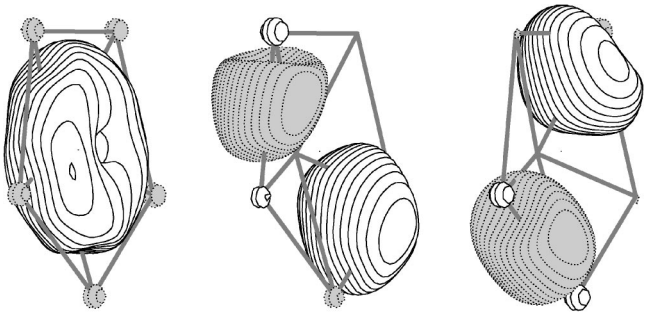

FIG. 9. HOMO-2, HOMO-1, and HOMO for the C_{5v} isomer of Li_6.

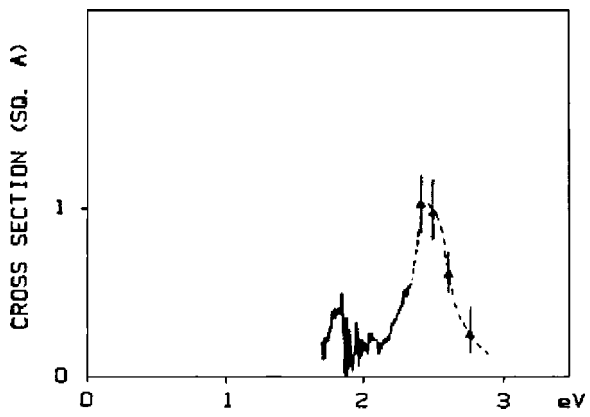

FIG. 11. Optical absorption spectrum of Li_6 (Refs. 4 and 6) with peaks at 1.8 and 2.5 eV. Reprinted figure with permission from Dugourd *et al.*, Phys. Rev. Lett. **67**, 2638 (1991). Copyright 1991 by the American Physical Society.

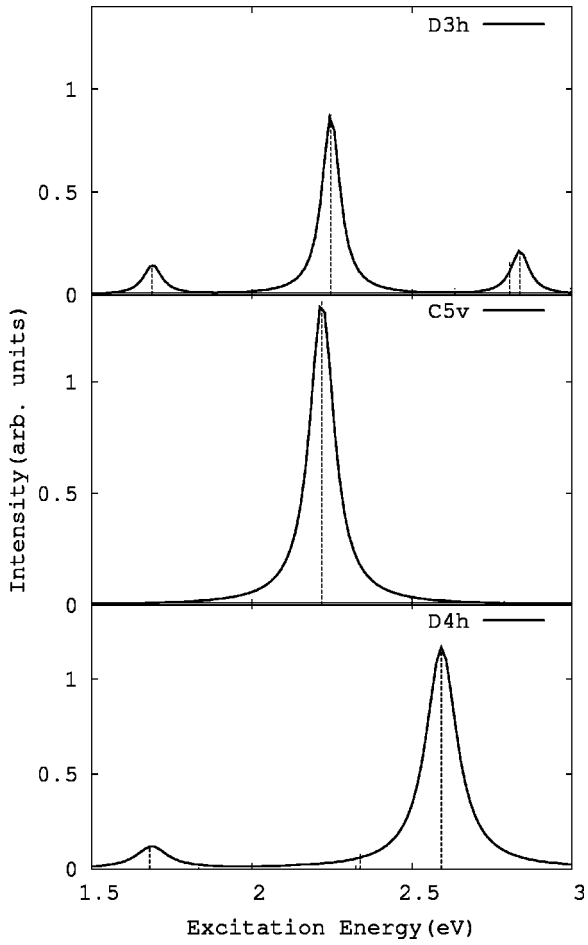

FIG. 12. Calculated vertical absorption spectra for three isomers of Li_6 (lines broadened artificially to facilitate comparison).

basis set dependence of the energetics (as seen in Tables I and III) geometries reported by Rousseau[11] compare favorably with the present CCSD(T)/cc-pCVQZ geometries, which usually exhibit slightly longer ($\approx$0.02–0.03 Å) bonds. The greatest difference is seen for the C_{5v} isomer, where the QCISD/6-311G* bond lengths (D_1=2.867 Å, D_2=3.151 Å) differ significantly from those at the more complete CCSD(T)/cc-pCVQZ level (D_1 =2.834 Å, D_2=3.113 Å).

D. Higher-spin states

Although it is understood that the ground state of Li_6 is a singlet, we investigated the possible presence of low-lying minima with higher spin multiplicities. We attempted first to locate higher-spin states with the same point group symmetries observed for the ground state minima: D_{4h}, C_{5v}, and D_{3h}. Table IV summarizes the results. Vibrational frequency analysis indicates that none of the stationary points obtained for these higher-spin states are potential energy minima; in each case, the number of imaginary vibrational frequencies (the Hessian index) is at least one, indicating a saddle point on the potential energy surface. Although we attempted to follow the imaginary frequency modes downhill to locate true minima, the high-spin computations in lower symmetries were plagued with convergence difficulties; as these states were not of prime interest for our current purposes, we did not pursue optimization further except for a triplet state discussed below.

Several of the stationary points in Table IV are fairly close in energy to the singlet states. For the D_{4h} configuration, the next triplet state is 8 kcal mol^{-1} higher in energy at

TABLE IV. Higher-spin states of the neutral Li_6.

Level of theory	$2S+1$	Energy (a.u.)	Bond length (Å) D_1	Bond length (Å) D_2	ZPVE[a]	Relative energy[a,b]	Hessian index[c] (Imag. Freqs.)
D_{4h}							
CCSD(T)/cc-pCVDZ	1	−44.983 317	2.699	2.848	3.71	0.00	0
CCSD(T)/cc-pCVDZ	3	−44.971 288	4.756	2.893	3.05	7.55	2(117,117)
CCSD(T)/cc-pCVDZ	5	−44.939 902	3.996	2.951	3.16	27.24	3(365,217,217)
C_{5v}							
CCSD(T)/cc-pCVDZ	1	−44.976 566	2.865	3.148	3.23	0.00	0
CCSD(T)/cc-pCVDZ	3	−44.946 166	3.055	2.920	3.00	19.62	2(99,99)
CCSD(T)/cc-pCVDZ	5	−44.921 427	3.130	2.933	2.66	34.60	8[d]
D_{3h}							
CCSD(T)/cc-pCVDZ	1	−44.974 510	2.983	3.089	3.21	0.00	0
CCSD(T)/cc-pCVDZ	3	−44.931 200	3.096	2.957	2.56	27.18	2(761,88)
CCSD(T)/cc-pCVDZ	5	−44.893 733	3.048	2.778	3.20	50.69	2(46,46)
C_{2v} Minimum							
CCSD(T)/cc-pCVDZ	3	−44.975 617	2.957	2.929–3.023	3.73	4.83	0

[a]In kcal mol^{-1}.
[b]Energy relative to the singlet state with the same point-group symmetry at the same level of theory (neglecting ZPVE).
[c]Number of imaginary frequencies, with the magnitude of those frequencies (cm^{-1}) in parentheses.
[d]Imaginary frequencies not listed.

TABLE V. Geometries and properties of Li_6^+ and Li_6^-.

			Binding energy[a]		
Molecule/symmetry	Level of theory	Energy (a.u.)	Total	Per atom	ZPVE[a]
Li_6^+/C_s	CCSD(T)/cc-pCVDZ	−44.826 482	142.55	23.76	3.60
Li_6^-/D_{4h}	CCSD(T)/cc-pCVDZ	−45.015 643	126.81	21.14	3.73
Li_6^-/D_{4h}	CCSD(T)/cc-pCVDZ+diff[b]	−45.016 307	124.14	20.69	3.73

[a]In kcal mol^{-1}.
[b]cc-pCVDZ with *s* and *p* diffuse functions from the 6-311++G** basis.

the CCSD(T)/cc-pCVDZ level of theory. The lowest triplet surface remains within 20 and 27 kcal mol^{-1} for the C_{5v} and D_{3h} configurations, respectively, at this level. Quintet states are somewhat higher in energy (27–51 kcal mol^{-1}), and septets are higher still. As indicated in the table, the geometrical parameters for these higher-spin stationary points can change substantially (e.g., by 2.057 Å for D_1 in the D_{4h} triplet).

Unfortunately, our limited investigations of lower-symmetry geometries for these higher spin states yielded only a $^3B_1$ minimum structure of C_{2v} symmetry. This triplet was also predicted by Boustani *et al.*[24] who used SCF and MRD-CI methods with 6-31G basis to locate this structure and characterize it as a minimum using normal mode analysis. The geometric parameters for this triplet state are given in Fig. 4. Compared to the singlet D_{4h} isomer, the C_{2v} triplet has a significantly longer axial bond length of 2.957 Å, and the bonds extending from the atoms on the axis to those on the central plane are also considerably longer (2.929–3.023 Å) than the 2.848 Å predicted for the D_{4h} singlet at the CCSD(T)/cc-pCVDZ level. This C_{2v} triplet is only 4.83 and 0.60 kcal mol^{-1} above the D_{4h} and C_{5v} singlet isomers, respectively, and 0.69 kcal mol^{-1} below the singlet D_{3h} isomer at the CCSD(T)/cc-pCVDZ level. Boustani *et al.*[24] also found triplet structures of C_{5v} ($^3E_1$) and D_{3h} ($^3E'$) symmetries lying only 4–5 kcal mol^{-1} above the singlets using the SCF and MRD-CI methods with minimal basis set, but normal mode analysis was not done to confirm if they were actual minima.

E. Li_6^+

Unlike the neutral hexamer, only one structure has been reported for the cation. Minimal basis set SCF and MRD-CI computations by Boustani *et al.*[24] found a D_{2h} structure with binding energies per atom of 12.24 kcal mol^{-1} (SCF) and 19.41 kcal mol^{-1} (Davidson-corrected MRD-CI). Our CCSD(T)/cc-pCVDZ indicate a less symmetric structure with C_{2v} symmetry. Figure 5 and Table V describe the geometric parameters and properties of Li_6^+. The structure is perhaps best thought of as a distortion which eliminates the C_4 axis of the the axially-compressed D_{4h} isomer of the neutral. The axial bond is shortened by a modest amount, 0.079 Å at the CCSD(T)/cc-pCVDZ level, while the other bonds change dramatically as a result of the ionization: bonds extending from the axial atoms to the atoms in the central plane change from ~2.8 Å for Li_6 to ~3.0–3.1 Å for Li_6^+. The distortion is a manifestation of the Jahn-Teller effect; in the D_{4h} geometry, Li_6^+ contains doubly degenerate HOMO orbitals which are not both doubly occupied, and the energy may be lowered by a distortion of the structure which breaks that degeneracy. We note that the cation is more stable to atomization (to 5 Li+Li^+) than any of the neutral isomers (to 6 Li). Its atomization energy of 1.03 eV (23.76 kcal mol^{-1}) agrees well with the experimental value of 1.08 eV found by Bréchignac *et al.*[17]

The adiabatic ionization energies at the CCSD(T)/cc-pCVDZ level are 4.27, 4.08, and 4.03 eV for the D_{4h}, C_{5h}, and D_{3h} isomers, respectively. Experimental ionization potential (IP) for Li_6 (Refs. 16, 61, and 62) have been determined by linear extrapolation of photoionization efficiency curves, yielding an IP that lies between the adiabatic and vertical limits. Nevertheless, the experimental IP of 4.20 eV compares favorably with the calculated adiabatic IP for the D_{4h} isomer, even though the estimated error of ±0.1 eV in our values, as well as the absence of pure adiabatic IP from experiment, makes the comparison less robust.

F. Li_6^-

The anion, like the cation, has not been studied extensively. Minimal basis SCF and MRD-CI computations indicate a single structure of D_{4h} symmetry.[24] Our CCSD(T)/cc-pCVDZ computations also yield a D_{4h} structure. Figure 6 and Table V present our results for the geometry and energetics of Li_6^-. As mentioned previously, diffuse functions can be critical for anions, and so we have compared results with the cc-pCVDZ basis to the cc-pCVDZ+diff basis described above. In this case, geometries and binding energies do not change dramatically upon the addition of diffuse functions.

Relative to the D_{4h} isomer of the neutral Li_6, the anion is less oblate; the ratio of its rotational constant with respect to the nondegenerate axis (0.108 cm^{-1}) to the degenerate axes (0.146 cm^{-1}) is only 1.352 at the CCSD(T)/cc-pCVDZ+diff level of theory, compared to a CCSD(T)/cc-pCVDZ value of 1.542 for the neutral cluster. The axial bond length is significantly larger (3.259 Å versus 2.699 Å) compared to the neutral cluster. On the other hand, the bonds extending from from the axial atoms to the equatorial atoms change very sightly from the neutral D_{4h} structure—from 2.813 Å for Li_6 to 2.872 Å for Li_6^-. The anionic cluster is more stable against dissociation (to 5 Li+Li^-) than the neutral cluster (to 6 Li), by a difference of 6.69 kcal mol^{-1} using the CCSD(T)/cc-pCVDZ+diff binding energy for Li_6^-. The adiabatic electron affinities for the D_{4h}, C_{5v}, and D_{3h} structures of Li_6 are estimated as 0.89, 1.07, and 1.13 eV at the CCSD(T)/cc-pCVDZ+diff level without ZPVE correction.

IV. CONCLUSIONS

The Li_6^+, Li_6^- clusters and three isomers of Li_6 have been studied using CCSD(T) with large basis sets and their optimum geometries and energetics have been reported. For the neutral cluster, the D_{4h} isomer is the most stable structure with a total atomization energy of 123.24 kcal mol^{-1}, as compared to 117.62 kcal mol^{-1} and 115.65 kcal mol^{-1} for the C_{5v} and D_{3h} isomers, respectively. This contrasts with other metal hexamers such as Na_6 and Au_6 which are thought to have a D_{3h} global minimum. Spectral features from experimental optical absorption spectra of Li_6 compare well with those from our EOM-CCSD vertical excitation spectra for the D_{4h} isomer, but not as well for the D_{3h} and C_{5v} isomers. There exist some low-lying states of higher spin multiplicity but none have a minimum structure of D_{4v}, C_{5v} or D_{3h} symmetry. A $^3B_1$ minimum of C_{2v} symmetry was found, lying 0.7 kcal mol^{-1} below the D_{3h} singlet minimum. For Li_6^+, the global minimum corresponds to a structure of C_{2v} symmetry, resulting from a stabilizing Jahn-Teller distortion. Its atomization energy is 142.55 kcal mol^{-1} at the CCSD(T)/cc-pCVDZ level. The anion, Li_6^-, has a D_{4h} structure and a total binding energy of 124.14 kcal mol^{-1} at the CCSD(T)/cc-pCVDZ+diff level of theory. Theoretical predictions for these clusters were found to be sensitive both to the basis set used and to electron correlation, including core correlation. The present, high-accuracy coupled-cluster results should help guide the interpretation of experiments on these clusters, which are at the size where 2D and 3D structures are energetically competitive.

ACKNOWLEDGMENTS

The authors would like to thank Professor Robert L. Whetten (Georgia Tech) and Steven Wheeler (University of Georgia) for helpful discussions. C.D.S. is a Blanchard Assistant Professor of Chemistry at Georgia Tech, and he acknowledges a National Science Foundation CAREER Award (Grant No. CHE-0094088) and a Camille and Henry Dreyfus New Faculty Award. The Center for Computational Molecular Science and Technology is funded through a Shared University Research (SUR) grant from IBM and by Georgia Tech.

[1] P. Ballone and W. Andreoni, *Metal Clusters* (Wiley, New York, 1999).
[2] M. Brack, Rev. Mod. Phys. **65**, 677 (1993).
[3] W. A. de Heer, Rev. Mod. Phys. **65**, 611 (1993).
[4] J. Blanc, V. Bonačić-Koutecký, M. Broyer, J. Chevaleyre, P. Dougard, J. Koutecký, C. Scheuch, J. P. Wolf, and L. Wöste, J. Chem. Phys. **96**, 1793 (1992).
[5] V. Bonačić-Koutecký, J. Pittner, C. Scheuch, M. F. Guest, and J. Koutecký, J. Chem. Phys. **96**, 7938 (1992).
[6] P. Dugourd, J. Blanc, V. Bonačić-Koutecký, M. Broyer, J. Chevaleyre, J. Koutecký, J. Pittner, J. P. Wolf, and L. Wöste, Phys. Rev. Lett. **67**, 2638 (1991).
[7] V. Bonačić-Koutecký, P. Fantucci, and J. Koutecký, Phys. Rev. B **37**, 4369 (1988).
[8] V. Bonačić-Koutecký, P. Fantucci, and J. Koutecký, Chem. Rev. (Washington, D.C.) **91**, 1035 (1991).
[9] J. Koutecký, I. Boustani, and V. Bonačić-Koutecký, Int. J. Quantum Chem. **38**, 149 (1990).
[10] R. Rousseau and D. Marx, Chem.-Eur. J. **6**, 2982 (2000).
[11] R. Rousseau and D. Marx, Phys. Rev. A **56**, 617 (1997).
[12] S. E. Wheeler, K. W. Sattelmeyer, P. v. R. Schleyer, and H. F. Schaefer III, J. Chem. Phys. **120**, 4683 (2004).
[13] W. D. Knight, K. Clemenger, W. A. de Heer, W. A. Saunders, M. Y. Chou, and M. L. Cohen, Phys. Rev. Lett. **52**, 2141 (1984).
[14] J. L. Martins, R. Car, and J. Buttet, Surf. Sci. **106**, 265 (1981).
[15] Z. Penzar and W. Ekardt, Z. Phys. D: At., Mol. Clusters **19**, 109 (1991).
[16] G. Gardet, F. Rogemond, and H. Chermette, J. Chem. Phys. **105**, 9933 (1996).
[17] C. Bréechignac, H. Busch, P. Cahuzac, and J. Leygnier, J. Chem. Phys. **101**, 6992 (1994).
[18] C. Yannouleas and U. Landman, Phys. Rev. Lett. **78**, 1424 (1997).
[19] C. Yannouleas and U. Landman, J. Chem. Phys. **107**, 1032 (1997).
[20] Y. Sakurai, Y. Tanaka, A. Bansil, S. Kaprzyk, A. T. Stewart, Y. Nagashima, T. Hyodo, S. Nanao, H. Kawata, and N. Shiotani, Phys. Rev. Lett. **74**, 2252 (1995).
[21] W. Schulke, G. Stutz, F. Wohlert, and A. Kaprolat, Phys. Rev. B **54**, 14381 (1997).
[22] M. W. Sung, R. Kawai, and K. H. Weare, Phys. Rev. Lett. **73**, 3552 (1994).
[23] R. O. Jones, A. I. Lichtenstein, and J. Hutter, J. Chem. Phys. **106**, 4566 (1997).
[24] I. Boustani, W. Pewestorf, P. Fantucci, V. Bonačić-Koutecký, and J. Koutecký, Phys. Rev. B **35**, 9437 (1987).
[25] A. Grassi, G. M. Lombardo, G. G. N. Angilella, N. H. March, and R. Pucci, J. Chem. Phys. **120**, 11615 (2004).
[26] M. J. McAdon and I. W. A. Goddard, Phys. Rev. Lett. **55**, 2563 (1985).
[27] M. J. McAdon and I. W. A. Goddard, J. Non-Cryst. Solids **75**, 149 (1985).
[28] M. J. McAdon and I. W. A. Goddard, J. Phys. Chem. **91**, 2607 (1987).
[29] P. Fantucci, V. Bonačić-Koutecký, J. Jellinek, M. Wiechert, R. J. Harrison, and M. F. Guest, Chem. Phys. Lett. **250**, 47 (1996).
[30] R. Rousseau and D. Marx, Phys. Rev. Lett. **80**, 2574 (1998).
[31] R. Rousseau and D. Marx, J. Chem. Phys. **111**, 5091 (1999).
[32] Y. Ishikawa, Y. Sugita, T. Nishikawa, and Y. Okamoto, Chem. Phys. Lett. **333**, 199 (2001).
[33] A. Ishii, K. Ohno, Y. Kawazoe, and S. G. Louie, Phys. Rev. B **65**, 245109 (2002).
[34] S. K. Lai, P. J. Hsu, K. L. Wu, W. K. Liu, and M. Iwamatsu, J. Chem. Phys. **117**, 10715 (2002).
[35] K. J. Taylor, C. Jin, J. Conceicao, L. Wang, O. Cheshnovsky, B. R. Johnson, P. J. Nordlander, and R. E. Smalley, J. Chem. Phys. **93**, 7515 (1990).
[36] K. Balasubramanian and D. Liao, J. Chem. Phys. **94**, 5233 (1991).
[37] D. Liao and K. Balasubramanian, J. Chem. Phys. **97**, 2548 (1992).
[38] H. Hakkinen and U. Landman, Phys. Rev. B **62**, R2287 (2000).
[39] G. Mills, M. S. Gordon, and H. Metiu, J. Chem. Phys. **118**, 4198 (2003).
[40] C. Massobrio, A. Pasquarello, and A. D. Corso, J. Chem. Phys. **109**, 6626 (1998).
[41] C. Massobrio, A. Pasquarello, and A. D. Corso, Chem. Phys. Lett. **238**, 215 (1995).
[42] I. A. Solov'yov, A. V. Solov'yov, and W. Greiner, Phys. Rev. A **65**, 053203 (2002).
[43] K. Raghavachari, J. A. Pople,G. W. Trucks, and M. Head-Gordon, Chem. Phys. Lett. **157**, 479 (1989).
[44] J. F. Stanton, J. Gauss, W. J. Lauderdale, J. D. Watts, and R. J. Bartlett, ACES II, the package also contains modified versions of the MOLECULE Gaussian integral program of J. Almlöf and P. R. Taylor, the ABACUS integral derivative program written by T. U. Helgaker, H. J. Aa. Jensen, P. Jørgensen, and P. R. Taylor, and the PROPS property evaluation integral code of P. R. Taylor.
[45] MOLPRO 2002.6 is a package of *ab initio* programs designed by H.-J. Werner and P. J. Knowles, with contributions from R. D. Amos, A. Bernhardsson, A. Berning *et al.*
[46] G. Schaftenaar and J. H. Noordik, J. Comput.-Aided Mol. Des. **14**, 123 (2000).
[47] J. F. Stanton and R. J. Bartlett, J. Chem. Phys. **98**, 7029 (1993).
[48] T. J. Lee, J. E. Rice, G. E. Scuseria, and H. F. Schaefer, Theor. Chim. Acta **75**, 81 (1989).
[49] T. J. Lee and P. R. Taylor, Int. J. Quantum Chem., Quantum Chem. Symp. **23**, 199 (1989).
[50] T. H. Dunning Jr., J. Chem. Phys. **90**, 1007 (1989).
[51] D. E. Woon and T. H. Dunning, Jr., J. Chem. Phys. **103**, 4572 (1995).
[52] A. K. Wilson, T. V. Mourik, and T. H. Dunning, Jr., J. Mol. Struct.: THEOCHEM **388**, 339 (1996).
[53] R. A. Kendall, T. H. Dunning, Jr., and R. J. Harrison, J. Chem. Phys. **96**, 6796 (1992).

[54]2002 basis sets were obtained from the Extensible Computational Chemistry Environment Basis Set Database, Version 7/29/02, as developed and distributed by the Molecular Sciences Computing Facility, Environmental and Molecular Sciences Laboratory (EMSL), which is a part of Pacific Northwest National Laboratories, P.O. Box 999, Richland, Washington 99352 and funded by the U.S. Department of Energy. The Pacific Northwest Laboratory is a multiprogram laboratory operated by Battelle Memorial Institute for the U.S. Department of Energy under Contract No. DE-AC06-76RLO 1830. Contact David Feller or Karen Schuchardt for more information.
[55]M. A. Iron, M. Oren, and J. M. L. Martin, Mol. Phys. **101**, 1345 (2003).
[56]K. A. Peterson and T. H. Dunning, Jr., J. Chem. Phys. **117**, 10548 (2002).
[57]R. Krishnan, R. S. J. S. Binkley, and J. Pople, J. Chem. Phys. **72**, 650 (1980).
[58]H. B. C. Bréchignac, P. Cahuzac, and J. Leygnier, J. Phys. Chem. **101**, 6992 (1994).
[59]B. Temelso, E. F. Valeev, and C. D. Sherrill, J. Phys. Chem. A **108**, 3068 (2004).
[60]J. L. Martins, J. Buttet, and R. Car, Phys. Rev. B **31**, 1804 (1985).
[61]P. Dugourd, D. Rayane, P. Labastie, B. Vezin, J. Chevaleyre, and M. Broyer, Chem. Phys. Lett. **197**, 433 (1992).
[62]B. Vezin, P. Dugourd, D. Rayane, P. Labastie, J. Chevaleyre, and M. Broyer, Chem. Phys. Lett. **206**, 521 (1993).